International Journal of Latest Trends in Engineering and Technology
Special Issue - International Conference on Nanotechnology: The Fruition of Science-2017, *pp.066-069*
e-ISSN:2278-621X, p-ISSN: 2319-3778

EXPERIMENTAL (FT-IR & FT-RAMAN) AND THEORETICAL (DFT) STUDIES OF VIBRATIONAL AND MOLECULAR STRUCTURE OF METHYL 2-(N-(2-METHOXY ACETYL)-2,6-DIMETHYL ANILINO) PROPANOATE

G.P. Sheeja Mol[1], D. Aruldhas[2]

Abstract- A combined studies were conducted on the molecular structure and vibrational spectra of methyl 2-(N-(2-methoxy acetyl)-2,6-dimethyl anilino) propanoate . The FT-IR and FT-Raman spectra of title compound were recorded in the ground state have been calculated by using the DFT methods using 6-311G(d, p) basis set. The optimized parameters (bond lengths, bond angles and dihedral angles) obtained by DFT method shows good agreement with the experimental values. Natural bond orbital analysis has been carried out to explain the charge transfer or delocalization of charge due to the intra molecular interactions. The energy of the highest occupied molecular orbital (HOMO) and lowest unoccupied (LUMO) molecular orbital have been predicted.
Keywords: methyl 2-(N-(2-methoxy acetyl)-2,6-dimethyl anilino) propanoate, FT-IR, FT-Raman

I. INTRODUCTION

Methyl N-(methoxyacetyl)-N-(2,6-xylyl)-DL-Alaninate (Metalaxyl) is a phenyl amide fungicide with systemic function. It can be used to control pythium in a number of vegetable crops and phytophthora in peas[1]. The enantiomerization and enantioselective bioaccumulation of metalaxyl in Tenebrio Molitor larvae were explained by Y.Gao etal[2]. Virginia Perez-Fernandez et al. reported the chiral separation of metalaxyl and benalaxyl fungicides by electrokinetic chromatography and determination of enantiomeric impurities [3]. Structural and spectroscopic analysis has been performed using computation and experimental methods. Fig 1 represents the molecular structure of methyl N-(methoxyacetyl)-N-(2,6-xylyl)-DL-Alaninate.

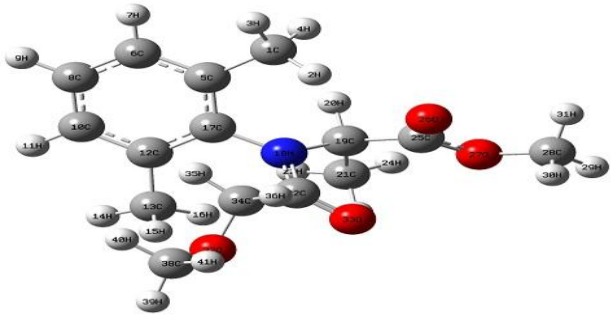

Fig 1: molecular structure of methyl N-(methoxyacetyl)-N-(2,6-xylyl)-DL-Alaninate

II. Experimental details

Methyl N-(methoxyacetyl)-N-(2,6-xylyl)-DL-Alaninate was purchased from Sigma Aldrich (St. Louis, MO, USA) and used without further purification. The FT-IR spectra of the title compound were measured in the region 400-4000 cm^{-1} using Perkin Elmer spectrometer equipped with mercury vapor lamp and globar as the source. The FT-Raman spectrum in the range 50-3500 cm^{-1} was also recorded on Bruker RFS 27 FT-Raman spectrometer.

III. Computational details

Gaussian 09software program package was used for theoretical calculation [4]. The quantum chemical calculations were performed by applying density functional theory method with the three parameter hybrid functional (B3) for the exchange part and the Lee-Yang-Par (LYP) correlation function . The wave number values computed contain known systematic errors and therefore, scaling factor 0.9682 [5] has been used. The potential energy distribution (PED) was calculated with the help of VEDA 4 program package [6].The Raman activities (S_i) calculated by Gaussian 09 program has been converted to relative Raman intensities (I_i) using the following relationship derived from the basic theory of Raman scattering [7].

[1] *Department of physics, NMCC Marthandam, Kanyakumari district, Tamilnadu, India*
[2] *Department of physics, NMCC Marthandam, Kanyakumari district, Tamilnadu, India*

$$I_i = \frac{f(\nu_o - \nu_i)^4 S_i}{\nu_i[1-\exp(-hc\nu_i/k_bT)]}$$

where ν_0 is the exciting wave number, ν_i the vibrational wave number of the normal mode, h, c and k_b are the universal constants and f is the suitably chosen common normalization factor for all the peak intensities. The natural charges of the atoms of compound 1 and its related compound was determined by NBO analysis using B3LYP/6-311G(d, p) method. Gauss view 5.0.8 visualization program [8] has been utilized to the shape of highest occupied molecular orbital (HOMO) and lowest unoccupied molecular orbital (LUMO).

Results and discussion

IV. Structural Analysis

The computed and experimental x-ray diffraction data are given in Table 1

Table 1: Optimized parameters

Bondlength(Å)			Bond angle(^{0})			Dihedral angle(^{0})		
	Expt.	Comput.		Expt.	Comput.		Expt.	Comput.
C_{17}-N_{18}	1.439	1.443	C_5-C_{17}-N_{18}	120.0	119.5	C_5-C_{17}-N_{18}-C_{19}	115.6	-73.9
N_{18}-C_{32}	1.350	1.379	C_{12}-C_{17}-N_{18}	121.0	119.4	C_5-C_{17}-N_{18}-C_{32}	-72.7	114.4
N_{18}-C_{19}	1.465	1.477	C_{17}-N_{18}-C_{32}	122.2	124.2	C_{12}-C_{17}-N_{18}-C_{32}	106.9	-66.4
C_{17}-C_5	1.392	1.408	C_{17}-N_{18}-C_{19}	122.2	118.4	C_5-C_{17}-N_{18}-C_{19}	115.6	-73.9
C_{17}-C_{12}	1.397	1.411	C_{19}-N_{18}-C_{32}	115.2	116.7	C_{12}-C_{17}-N_{18}-C_{19}	-64.8	105.2
O_{27}-C_{28}	1.454	1.439	N_{18}-C_{32}-O_{33}	122.8	121.6			

The N_{18}-C_{32} bondlength elongated 0.029Å due to the hyperconjugation interaction between N_{18}-C_{32}. In O_{27}-C_{28} the bondlength contracted 0.015Å due to the interaction between H_{30}….O_{27}. The dihedral angle reveals the nonplanarity of the title compound.

V. Vibrational spectral analysis

The vibrational spectra were analyzed based on the FT-IR spectra aswellas the vibrational wavenumbers computed at the DFT level with the scaled wavenumbers. The FT-IR spectra are given in Fig 2. IR spectral analysis is based on the vibrational modes of phenylring vibrations, methyl group vibrations, carbonyl group vibrations, C-N vibrations and C-O vibrations. The amide band due to the C=O stretching vibration is often referred to as the amide 1 band. Primary amides have a very strong band due to the C=O stretching at 1670-1650 cm^{-1}[9]. The IR spectrum shows a very strong band at 1686 cm^{-1} (PED 85%) which correspond the carbonyl group C=O stretching.

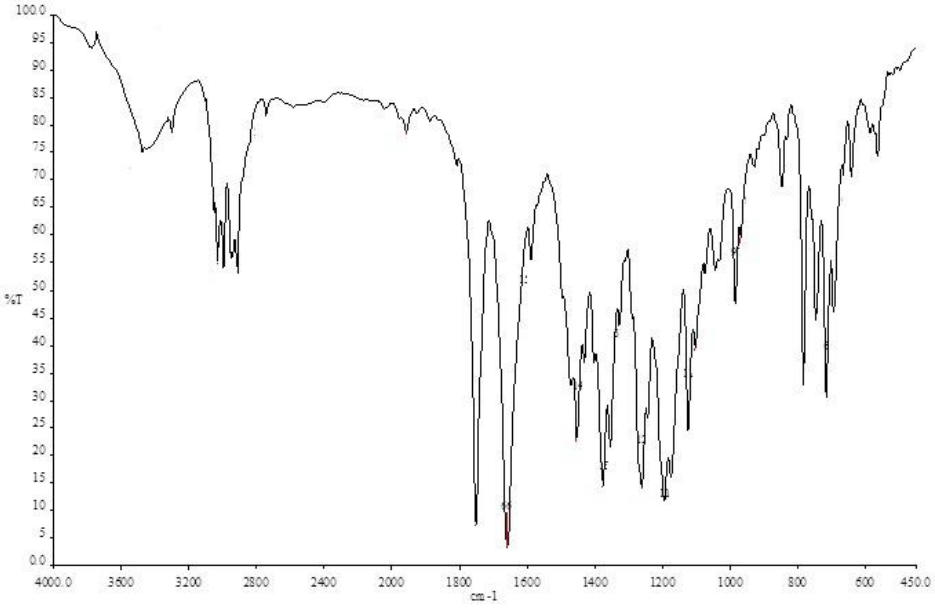

Fig 2: FT-IR spectrum of methyl N-(methoxyacetyl)-N-(2,6-xylyl)-DL-Alaninate

VI. NBO Analysis

The natural bond orbitals (NBO) calculations were performed using NBO 3.1 program [10] as implemented in the Gaussian 09 package at the DFT/B3LYP level. The NBO analysis is a tool for understanding hydrogen bonding interactions and delocalization of electron density from occupied donor and unoccupied acceptor within the molecule. The second order Fock-matrix was carried out to evaluate the donor-acceptor interactions in the NBO basis. The interactions result in a loss of

occupancy from the localized NBO of the idealized Lewis structure into an empty non-Lewis orbital. For each donor (i) and acceptor (j) the stabilization energy $E^{(2)}$ associated with the delocalization i→j determined as

$$E(2) = \Delta E_{ij} = q_i \frac{F(i,j)^2}{E_i - E_j}$$

In NBO analysis large $E^{(2)}$ value shows the intensive interaction electron donors and electron-acceptors, and greater the extent of conjugation of the whole system, the possible intensive interaction are given in Table 2. The second order perturbation theory analysis of Fock matrix in NBO basis shows strong intramolecular interactions of electrons.

Table 2: Second order perturbation theory Analysis

Compound	Donor NBO(i)	E.D/e	Acceptor NBO(j)	E.D/e	$E^{(2)}$ (kJ/mol)
Metalaxyl	$\sigma_{(C5-C6)}$	1.970 -0.687	$\sigma^*_{(C17-N18)}$	0.039 0.394	20.29
	$\sigma_{(C5-C17)}$	1.967 -0.692	$\sigma^*_{(C12-C17)}$	0.037 0.565	22.55
	$\sigma_{(C10-C12)}$	1.970 -0.689	$\sigma^*_{(C17-N18)}$	0.039 0.394	19.75
	$\sigma_{(C12-C17)}$	1.966 -0.690	$\sigma^*_{(C5-C17)}$	0.037 0.569	22.68
	$\sigma_{(C19-C25)}$	1.970 -0.638	$\sigma^*_{(O27-C28)}$	0.017 0.262	18.03

NBO analysis clearly manifests the evidence for the formation of H-bonded interactions between oxygen lonepair and $\sigma^*(C_1-H_4)$ antibonding orbital. The stabilization energy $E^{(2)}$ associated with strong hyperconjugation interactions $N_{18}\rightarrow\sigma^*(C_{19}-H_{20})$ is obtained as 9.99kJ/mol which quantify the extend of intramolecular hydrogen bonding in Table3. The difference in $E^{(2)}$ energies are reasonably due to the fact that the accumulation of electron density in the C-H bond is noticed as 2.88e. The strengthening and contraction of C-O bonds due to hybridisation are revealed by the low value of electron density 0.017e in the $\sigma^*(O_{27}-C_{28})$ orbitals as tabulated. The formation of intra molecular C-H...O hydrogen bonding interaction in compound is due to the presence of phenyl amide and the alaninate group, which is very important in the enhancement of the biological activity of this compound.

Table 3 : Possible hydrogen bonding of title compound

Compound	Donor NBO(i)	E.D/e	Acceptor NBO(j)	E.D/e	$E^{(2)}$ kJ/mol	H...O	D-H (Å)	H...A (Å)	D...A (Å)	D-H...A (^{0})
Metalaxyl	O_{26}	1.841 -0.262	$\sigma^*_{(C1-H2)}$	0.009 0.344	4.30	$sp^{3.08}$	1.088	2.393	3.315	141.5
	O_{26}	1.841 -0.262	$\sigma^*_{(C28-H29)}$	0.009 0.344	3.22	$sp^{3.08}$	1.087	3.700	2.645	11.8
	O_{27}	1.964 -0.562	$\sigma^*_{(C21-H22)}$	0.007 0.414	2.47	$sp^{3.28}$	1.091	3.769	2.707	11.2
	O_{33}	1.853 -0.251	$\sigma^*_{(C19-H20)}$	0.020 0.404	2.93	$sp^{3.78}$	1.094	3.733	2.698	15.9
	O_{33}	1.853 -0.251	$\sigma^*_{(C34-H35)}$	0.020 0.404	2.30	$sp^{3.78}$	1.100	2.648	2.389	64.4

The increased electron density at the oxygen atom (O_{26}) leads to the elongation of the C_{28}-H_{29} bond. The electron density is transferred from $n(O_{26})\rightarrow \sigma^*(C_1-H_2)$ showing 1.841e→0.009e which leadsto the high interaction energy (4.30kJ/mol). The intramolecular charge transfer is one of the causes for fungicidal activity of the compound1. The $n(O_{33})\rightarrow \sigma^*(C_{19}-H_{20})$ which indicates the lowest interaction energy 2.93kJ/mol which represent the weak intramolecular hydrogen bonding. These charge transfer interactions of a compound are responsible for the fungicidal activity.

VII. HOMO-LUMO analysis

Molecular orbitals, both the highest occupied molecular orbital (HOMO) and the lowest unoccupied molecular orbital (LUMO) and their properties of the HOMO are directly related to the ionization potential, LUMO energy is directly related to the electron affinity [11,12]. This is also used by the frontier electron density for predicting the most reactive position in p-electron systems and also explains several types of reaction in conjugated system [13]. The conjugated molecules are characterized by a small highest occupied molecular orbital-lowest unoccupied molecular orbital separation, which is the

result of a significant degree of intramolecular charge transfer from the end-capping electron-donor groups to the efficient electron-acceptor group through the p-conjugated path. The energy difference between HOMO and LUMO orbital which is called as energygap is a critical parameter in determining molecular electrical transport properties because it is a measure of electron conductivity; calculated -0.15192eV . The plots of MOs are drawn and given in Figure 3. The positive phase is red and the negative one is green. According to Figure3, the HOMO a charge density localized over the phenylamide region of the entire molecule, but the LUMO is characterized by a charge distribution on the phenylring. The observed transition from HOMO to LUMO is n→π*. Moreover lower in the HOMO and LUMO energygap explains the eventual charge transfer interactions taking place within the molecule.

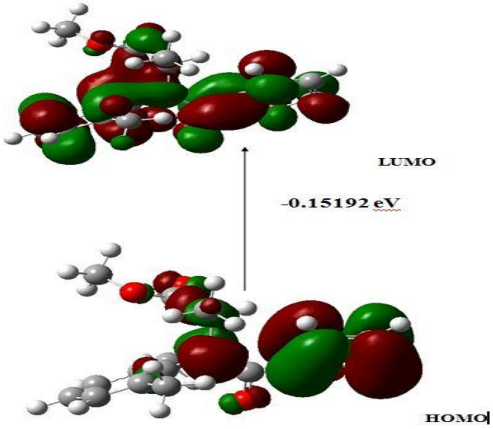

Figure 3: HOMO-LUMO Plot Conclusion

Vibrational wavenumbers and infrared intensities calculated by B3LYP/6-311G(d, p) level agrees well with the experimental data. The bondlength N_{18}-C_{32} increased due to the hyperconjugation interaction. NBO analysis shows that the intramolecular C_{19}-H_{20}…O_{33} hydrogen bond due to the interaction of the oxygen lonepair and the C-H antibonding orbital. The possibility of hydrogen bonding and charge transfer shows the fungicidal nature of title compound.

References

[1] O'Neil, M.J.(ed.). The Merck Index- An encyclopedia of chemicals, drugs and biological.13th edition, White house station, NJ:Merck and Co., Inc., 2001.,p.1058.
[2] Yongxin Gao, Hui weing, Fang qin, Peng xu, Xiatian LV, Jianzhong LI and Baayuan Gao, Chirality, 2014, 26, 88-94.
[3] Virginia Perez-Fernandez, Journal of Chromatography A, 2011,1218,4877-4885.
[4] M.J.Frisch.,etal., "Gaussian 09 revision", C.02, Gaussian InC Walling Ford, Ct, 2004.
[5] J.P.Merrick, D.Moran, L.Radom, J.Phys.Chem A 111(2007), 11683-11700
[6] M.H.Jamroz, vibrational energy distribution Analysis VEDA 4, warsaw, Poland (2004).
[7] G.Keresztury, S.Holly, J.V.Besengei, A.Y.Wang, Spectrochimica Acta Part A 49(1993), 2007-2026.
[8] R.Denningten, T.Keith, J.Millam, Gaussview version 5.0.8, Gaussian. Inc, 235 Wallingford CT, 2009.
[9] George Socrates, Infrared and Raman characteristic group frequencies, John Wiley & sons, Ltd, 3rd edition.
[10] E.D.Glendening, A.E.Reed, J.E.Carpenter, F.Weinhold, NBO Version 3.1, Gaussian InC. Pittsburgh, PA
[11] K.Fukui, Science218(1982) 747-754.
[12] S.Gunasekaran, R.A.Balaji, S.Kumaresan, G.Anand, S.Srinivasan, Can.J.Anal.Sci.Spectrosc.5 (2008), 149-162.
[13] K.Fukui, T.Yonezawa, H.Shingu, J.Chem.Phys.20 (1952), 722-725.